



OPEN High-efficiency dual-band switched beam antenna with back lobe suppression using parasitic elements and patch etching for 5G

Pichaya Chaipanya¹✉, Warisara Kongka¹, Nannaphat Wongpanyanurak¹, Chayangkun Wongplueksa¹, Natkamon Thongnuam¹, Waranya Suksaart¹, Khomdet Phapatanaburi², Samran Santalunai³ & Nuchanart Santalunai²✉

This paper presents the design and development of an innovative single-element, dual-band beam-switching antenna with back lobe suppression, tailored for 5G applications. The proposed antenna integrates parasitic elements and patch etching techniques to enhance performance while maintaining a compact and cost-efficient design. Operating effectively at 0.7 GHz and 2.6 GHz, the antenna features a square patch of 111.84 mm × 111.84 mm and a ground plane of 143.84 mm × 143.84 mm, optimized for dual-band performance. The design employs advanced techniques such as back lobe suppression, patch etching, and strategically placed short circuits, resulting in significant improvements in signal clarity and interference reduction. Simulations and measurement results confirm the antenna's ability to change its beam direction, allowing it to transition between 45°, 135°, 225°, and 315° angles. This enhances signal clarity, reduces interference, and boosts overall network reliability in dense urban environments. The results demonstrate outstanding beam-switching capabilities, with gains of 5.39 dBi at 0.7 GHz and 8.35 dBi at 2.6 GHz. This approach provides a robust solution for improving the coverage and reliability of 5G networks in extremely dense urban areas. This study offers valuable insights into antenna designs for future wireless technologies, providing a practical and cost-efficient solution with exceptional performance and seamless integration into existing systems.

Keywords Dual band, Switched beam, Back lobe, 5G mobile communication, Microstrip antennas

Wireless communication has become an essential and fundamental component of modern life, gaining even more importance with the advancement of 5G technology^{1–5}. Nowadays, the era of communication employs multiple frequency bands, each possessing unique attributes and uses. While mid-band frequencies, which span from 1 GHz to 6 GHz, offer greater speeds over a smaller area, low-band frequencies, which are under 1 GHz, provide substantial coverage but at slower rates. High-band frequencies, ranging from 24 GHz to 40 GHz, provide the fastest speeds but have limited coverage. Thailand's National Broadcasting and Telecommunications Commission has allocated frequencies of 0.7 GHz, 2.6 GHz, and 26 GHz for low band, mid band, and high band 5G applications, respectively. Deploying 5G involves important factors such as its restricted range and sensitivity to the changing propagation environment. These factors might affect the coexistence of other ISM wireless systems and impact the overall quality of communication.

In response to these difficulties, antenna arrays, which sacrifice some angular coverage, are being utilized more and more to improve signal propagation by combining several elements to produce a concentrated, high-gain beam. To address this constraint, smart antennas^{6–9} can be employed to provide a range of directed patterns that enhance the coverage of the system. Although achieving accurate beam steering typically involves using expensive and elaborate components, such as complex switching circuits or extensive digital signal processing, switched beam antennas offer a viable and cost-effective alternative^{10–12}. These antennas provide both reduced

¹Department of Electrical Engineering, Faculty of Engineering, Srinakharinwirot University, Ongkharak, Nakhon Nayok 26120, Thailand. ²Department of Telecommunication Engineering, Faculty of Engineering and Technology, Rajamangala University of Technology Isan, Nakhon Ratchasima 30000, Thailand. ³School of Electronic Engineering, Institute of Engineering, Suranaree University of Technology, Nakhon Ratchasima 30000, Thailand. ✉email: pichayac@g.swu.ac.th; nuchanart.fa@rmuti.ac.th

production and operational expenses, as well as enhanced scalability and energy efficiency. Their straightforward design facilitates seamless integration into preexisting systems, making them especially efficient in areas where precise control over signal intensity is crucial for ensuring reliable communication.

Switched beam antennas for 5G wireless communications come in various innovative designs, each enhancing network performance through different technological advancements. Notably, a high-band frequency antenna at 26 GHz features adjustable main beam directions at 0°, 45°, 90°, 135°, and 180° using phase shifters, as detailed in¹³. Another significant development is the switched parasitic array antenna described in¹⁴, which includes an active central element surrounded by parasitic elements that allow the main beam direction to be altered via switches. Further advancements are seen in dual-band switched beam antennas as described in¹⁵, where four-element patch antenna sub-arrays are strategically positioned on the sides of an octagonal prism, enabling beam steering by switching between sub-arrays. Moreover, multi-band capabilities are explored in^{16,17} with a design featuring a square split-ring resonator patch that operates across eight resonant frequencies from 7 GHz to 15 GHz and allows beam direction adjustments through a short circuit at different edges. The authors of¹⁸ introduce a cost-effective 28 GHz switched beam antenna for 5G, integrating a Butler matrix with a patch antenna to dynamically change beam directions. Achieving high gain and compact size, this design enhances 5G signal reliability and coverage, making it ideal for dense urban telecommunications. The authors of¹⁹ present a novel wideband beamforming antenna for 5G applications that eliminates the need for phase shifters and crossovers from the Butler matrix, simplifying design and reducing size. The antenna covers a significant bandwidth with low insertion loss, improving signal quality and reducing system complexity. Similarly, wideband endfire antenna arrays, as highlighted in²⁰, offer optimized designs for 5G mmWave mobile terminals, providing efficient beam steering and enhanced coverage in high-frequency bands.

While dual-band switched beam antennas are essential for 5G wireless communications, back lobes frequently present significant challenges^{21,22}. These can weaken the main beam's strength and introduce interference from undesired directions. Several research studies have investigated viable back lobe suppression methods to address these issues. One study significantly improves azimuth beam steering resolution by introducing an enhanced beam steering technique for circular switched parasitic array (SPA) antennas^{23,24}. The study identifies configurations that greatly enhance beam quality and direction through recurrent testing of various combinations of parasitic elements and associated impedance loads. This technique, extensively tested with an antenna prototype and validated through MATLAB and WIPL-D simulations, allows for more accurate control over beam direction in SPA antennas, potentially improving the performance of wireless communication systems. This research has inspired us to further utilize parasitic components to enhance the performance of dual-band switched beam antennas.

Moreover, concerning back lobe suppression techniques without using switched beam antennas, the incorporation of superstrates, reflecting surfaces, and frequency selective surfaces (FSS) into various antenna designs has shown promising results. For example, adding absorption chambers and air substrates to circular patch antennas with cylindrical copper wires and spiral antennas with directed radiation patterns has demonstrated notable decreases in back lobe levels²⁵. Furthermore, high-impedance surfaces on rectangular patch antennas are excellent at suppressing surface waves, which improves antenna performance without requiring intricate switching mechanisms²⁶. Back lobe levels have also been successfully reduced by alternative non-switching techniques, such as etching gaps in antenna ground structures, as demonstrated by the slotted ground choke technique²⁷. Other designs, including the 2 by 2 planar array antenna with divided feeding approaches²⁸ and the use of defective ground structures (DGS)²⁹, purposefully modify the ground plane to reduce back radiation³⁰, further enhancing these techniques. By carefully placing shorting pins in microstrip patch antennas, a new technique is introduced to direct the radiation pattern away from the user, significantly reducing the Specific Absorption Rate (SAR) while maintaining strong signal coverage³¹. Similarly, a high-performance 2 × 2 MIMO antenna employing a novel frequency selective surface (FSS) demonstrated significant improvements in gain, directivity, and back lobe suppression for sub-6 GHz 5G applications, making it an efficient solution for modern wireless networks³². These advancements represent a major step forward in optimizing antenna designs with static configurations and highlight the potential of these techniques to improve mobile and wearable technology applications. These designs maintain excellent performance levels while addressing the specific challenges faced by modern wireless communication networks. This work makes a significant contribution to the field by focusing on the combined application of shorting pins and parasitic elements to enhance antenna performance by reducing back lobe interference.

The creation of a novel single-element, dual-band switching beam antenna designed to meet the rigorous requirements of 5G wireless communications is described in this work. This concept is visually demonstrated in Fig. 1, which contrasts the radiation pattern of a conventional omnidirectional antenna with that of the proposed switched beam antenna with integrated back lobe reduction. The illustration highlights how the proposed design achieves focused radiation and reduced interference by eliminating unwanted energy in the opposite direction of the main beam. The key contributions of this study include:

- (1) An innovative antenna has been successfully created and implemented, functioning flawlessly in two crucial frequency bands: approximately 0.7 GHz for improved coverage and 2.6 GHz for increased data throughput. Its dual-band capability is essential for enabling a wide range of 5G applications.
- (2) Unlike conventional approaches^{33–35}, this study incorporates cutting-edge techniques to suppress back lobes, improving signal clarity and reducing interference. This includes:
 - Plastic Elements: These are deliberately incorporated to alter the electromagnetic field and improve beam direction.

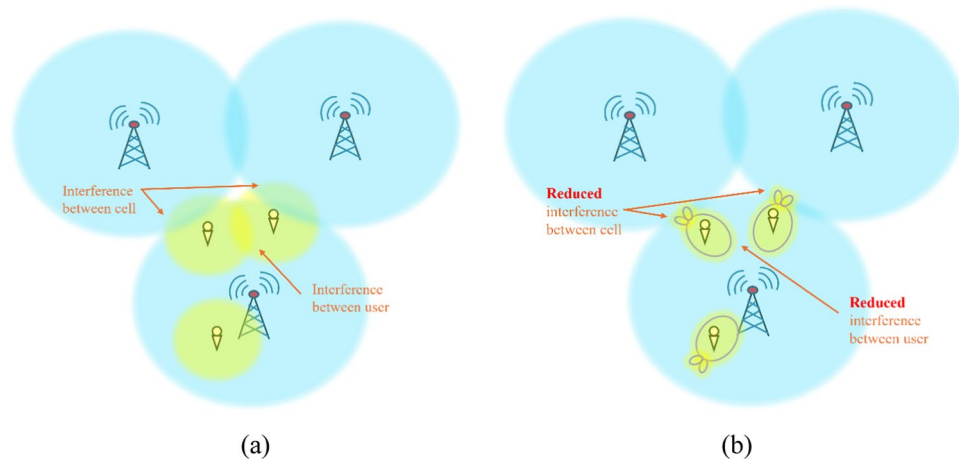


Fig. 1. Comparison between (a) a conventional omnidirectional antenna and (b) the proposed switched beam antenna with integrated back lobe reduction.

- Patch Etching: To modify the current distribution and help focus the beam and reduce energy waste in undesirable directions, we precisely etched the antenna patch.
 - Shorted Circuits: Located at precise locations, these circuits enable dynamic beam switching and direction fine-tuning, which are essential for 5G communication environments that are adaptable.
- (3) The antenna's design was thoroughly tested through a series of simulations and practical experiments, confirming its capacity to precisely steer beams in four distinct directions: 45°, 135°, 225°, and 315°. Additionally, the design demonstrated excellent beam-switching capabilities, which are crucial in dynamic metropolitan contexts for maintaining reliable communication. These tests confirm the antenna's outstanding performance, making it a reliable option for enhancing 5G network capabilities.

The rest of the paper is structured as follows: section “[Design and development of a single-element switched beam antenna with backlobe suppression techniques](#)” details the design and development of the proposed antenna. Section “[Comparative analysis and performance validation](#)” presents a comparative analysis and performance validation. Finally, section “[Conclusions](#)” provides the conclusion.

Design and development of a single-element switched beam antenna with backlobe suppression techniques

This section introduces the proposed antenna, which is designed to be assembled from three separate sections. The device is equipped with a dual-band microstrip square patch antenna, renowned for its ease of use and capacity to function at both 0.7 GHz and 2.6 GHz frequencies. These frequencies are crucial for 5G applications in Thailand. To improve directional communication capabilities, the design also incorporates a switched beam antenna that uses a shorted circuit technique. This technology allows for dynamic beam pattern alterations through the placement of shorted circuits in important locations. Additionally, a combination of patch etching methods, shorted circuits in four specified locations, and parasitic rings is used to address back lobe suppression. This method efficiently improves beam directionality and reduces back lobe radiation while preserving a simplified single-layer construction.

Dual-band microstrip square patch antenna design

The design of a dual-band microstrip square patch antenna in this work aims to enhance the performance described in³⁶, with a focus on operational optimization at the critical frequencies of 2.615 GHz and 0.705 GHz, which are essential for 5G deployments in Thailand. The square microstrip patch's geometric features are utilized in this design, where the width of each side is carefully tuned to resonate at these frequencies. The resonant frequency f_r of the patch is determined by the following fundamental equation³⁷:

$$f_r = \frac{c}{2L\sqrt{\epsilon_{eff}}} \quad (1)$$

where L is the patch's length, c is the speed of light in vacuum (3×10^8 m/s), and ϵ_{eff} is the substrate's effective permittivity, which takes into account both the substrate material's relative permittivity (ϵ_r) and the dielectric constant (ϵ). The equation is simplified to make practical calculations easier for substrates that are frequently used in 5G applications, such as FR4^{38,39}, which have a relative permittivity of 4.3. Assume that the substrate's relative magnetic permeability (μ_r), which is typical for non-magnetic materials used at RF frequencies, is close to unity.

$$f_r = \frac{c}{2L\sqrt{\varepsilon + 4.3}} \quad (2)$$

The antenna has a single patch with an inner part that is finely carved to enable dual-band operation^{40,41}. The patch's current distribution is significantly altered by this etching, making it capable of supporting a higher frequency. To achieve excellent impedance matching, the precise dimensions, such as the patch width and length, are carefully determined to enhance performance at the desired frequencies. This guarantees a uniform and balanced radiation pattern, which is ideal for consistent signal dissemination. The antenna employs a coaxial probe feeding mechanism, where the feed point is centrally located on the patch. This feed arrangement ensures a uniform distribution of the excitation signal, resulting in balanced current flow across the patch. The central feed point is chosen based on impedance matching considerations, which are crucial for minimizing reflection losses and achieving maximum power transfer. These crucial dimensions are illustrated in full in Fig. 2a, which depicts this efficient and compact design.

This research presents a significantly enhanced dual-band microstrip square patch antenna design that is specifically intended for large-scale fabrication and methodically optimized for important 5G frequencies. This antenna greatly advances next-generation wireless technology by integrating engineering theory with practical telecommunications requirements. The antenna's electromagnetic behavior and physical design are depicted in Fig. 2b, which also confirms resonance at 2.615 GHz and 0.705 GHz. The narrow slots play a crucial role in enhancing the performance of the antenna. These slots are carefully designed to improve the current distribution on the patch, which significantly influences the dual-band operation at 0.7 GHz and 2.6 GHz. By introducing the slots, the effective electrical length of the patch is modified, allowing the antenna to support two resonant frequencies within the desired bands. The *LC* equivalent circuit of the proposed etched patch antenna comprises a source denoting the feed point as illustrated in Fig. 2c, a parallel *LC* component (L_1, C_1) that models the patch's primary resonance at approximately 0.7 GHz, and a series capacitor C_s that represents the etched slots, which introduce a secondary resonance around 2.6 GHz. The ground (GND) represents the return path, corresponding to the antenna's physical ground plane. The figure also shows the current distributions supporting the antenna's dual-band capability, which is essential for 5G applications in Thailand. Figure 2d provides a detailed presentation of the current distribution information, which is essential for evaluating the antenna's performance.

Integration of shorted circuit techniques in switched beam antenna design

This component of the study discusses the management of the beam pattern, which is crucial for focused communication applications. It builds on the advancements discussed in the preceding section on the single element dual band microstrip square patch antenna. The antenna's utility in dynamic communication situations may be limited by the typical design's unadjustable beam direction.

Shorted circuits have been integrated at terminals on each patch, guided by the observed current distribution, to modify the main beam pattern. Notably, the patch's center has the strongest current, which steadily decreases toward the patch's borders in a pattern mostly controlled by the feed point in the middle, as seen in Fig. 2c. This central feed creates a stronger electric field and more concentrated current at the center of the patch by introducing electrical energy and designating it as the major zone for current distribution. There is less current at the patch's ambit because of the current's natural weakening as it spreads outward from this central feed. The way the feed point modifies the distribution of the electromagnetic field and current throughout the antenna is what causes this behavior. Two configurations of shorted circuits labeled case 1 and case 2 and shown in Fig. 3a are investigated in the context of this distribution. In Fig. 3a, the stubs are strategically introduced to enable the switching of the main beam direction. The number and location of these stubs were optimized through an iterative simulation process using CST Microwave Studio. This optimization focused on achieving precise beam direction control at 45°, 135°, 225°, and 315°, ensuring maximum directional gain while maintaining minimal interference. Various stub configurations were evaluated, with the final design offering the most effective beam-switching performance. The antenna's working frequencies are barely changed by these modifications, and both configurations show the same S_{11} values, indicating that the shorted circuit placements are symmetrically effective. Figure 3b and c show how different designs affect radiation patterns at 0.7 GHz and 2.6 GHz. The shorted places cause the radiation patterns to change, simulating the behavior of a directional antenna. In particular, the major beams point toward 45° and 225° in Case 2, while they target 135° and 315° in Case 1. The antenna was constructed using a single-layer printed circuit board with a FR4 substrate, which has a thickness of 1.6 mm and a dielectric constant of 4.3, to confirm its beam steering capabilities. At the patch center, a SMA connector was integrated from one side to the other. The performance of the antenna was confirmed by the simulation findings, which agreed with and supported by the measurement data. The shorted circuit approach validated this possibility.

Back lobe suppression strategies for dual-band switched beam antennas

The previous subsection clearly indicates that there are issues with the back lobe in the radiation pattern. To address this problem, we propose two distinct methods: incorporating parasitic rings and utilizing patch etching techniques. Strategically positioned parasitic elements surround the antenna's primary radiation patch. Without directly obtaining electricity, these rings serve as passive elements that affect the electromagnetic field surrounding the active radiating elements. We can successfully adjust the radiation pattern of the antenna to lower the intensity of back lobe radiation by carefully planning their placement and size^{42,43}. Using patch etching techniques, the antenna patch is etched directly with accurate patterns. The regions that are etched away modify the patch's current distribution, which modifies the radiation pattern. The design addresses suppression of undesired radiation directions, especially the back lobes, by selectively eliminating portions of the patch. This improves the antenna's overall directivity in addition to sharpening the main lobe⁴⁴.

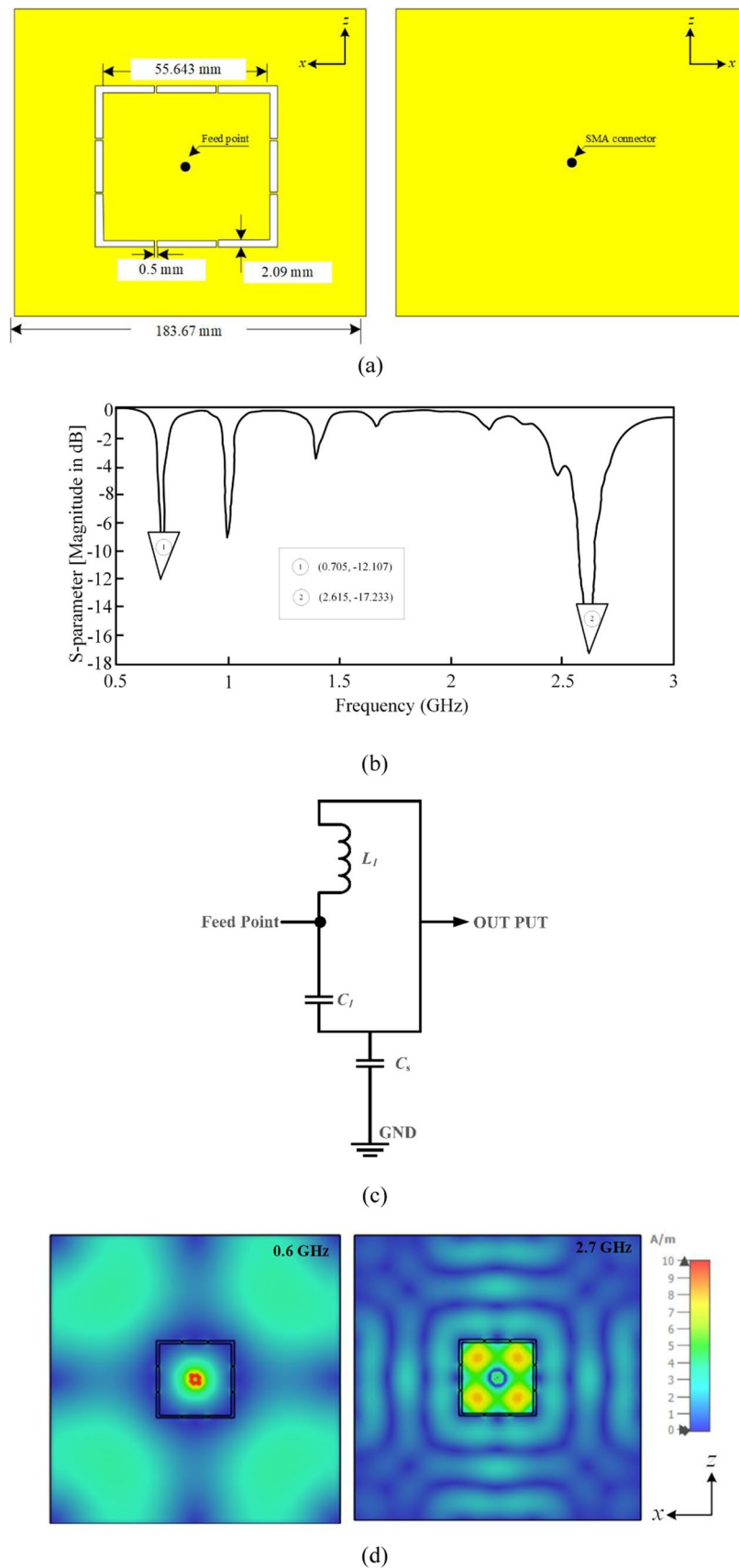


Fig. 2. Simulation of dual band microstrip square patch antenna (a) structure, (b) S_{11} , (c) LC equivalent circuit and (d) surface current.

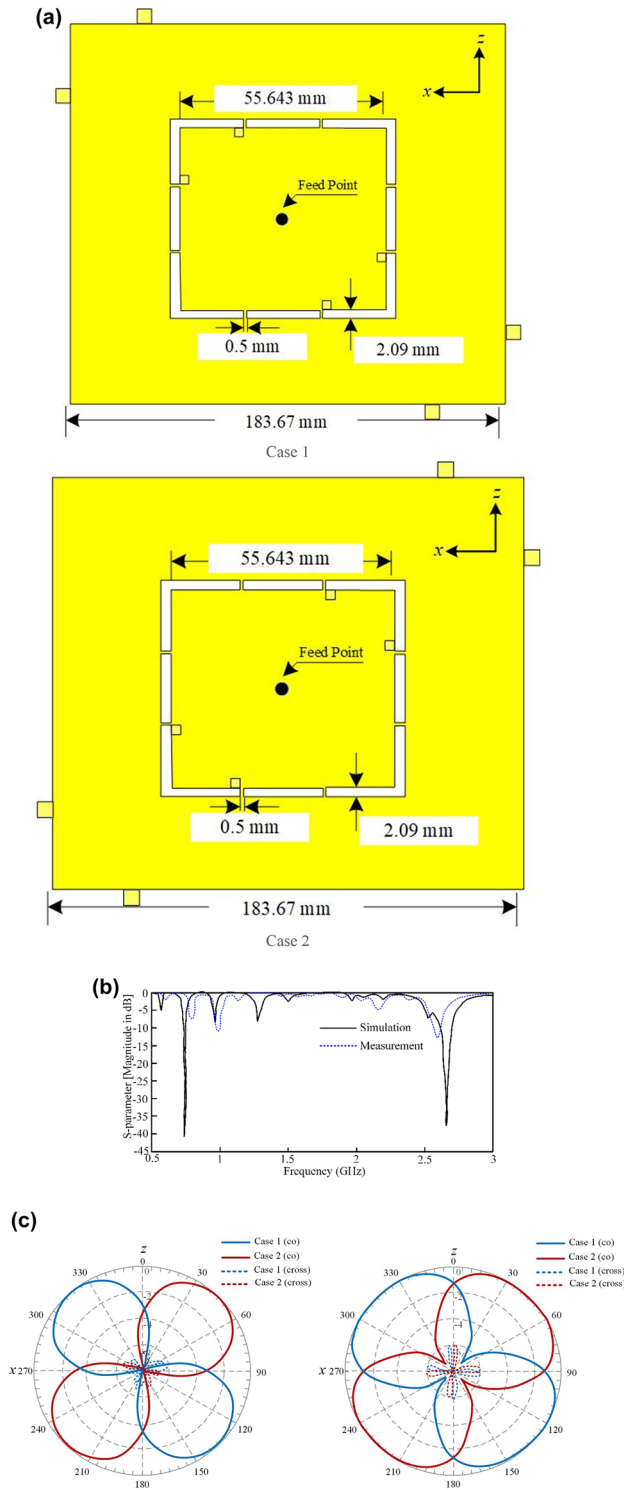
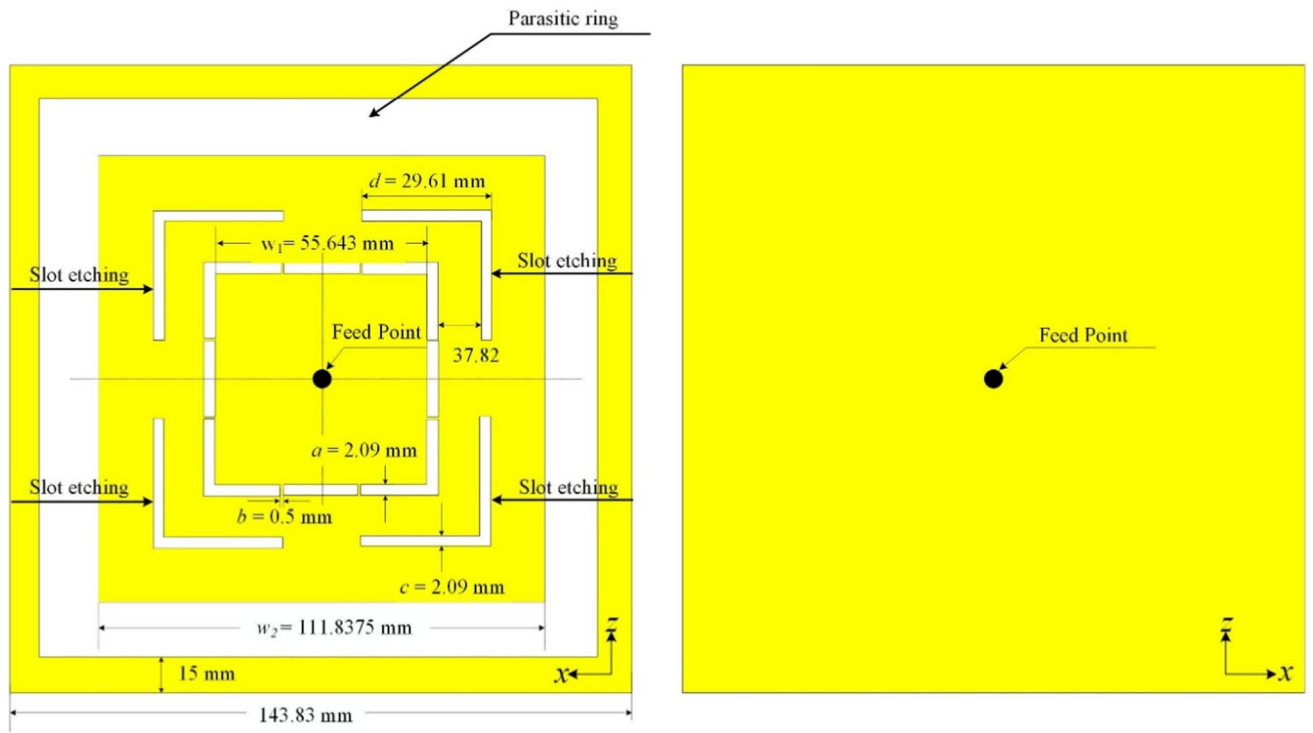
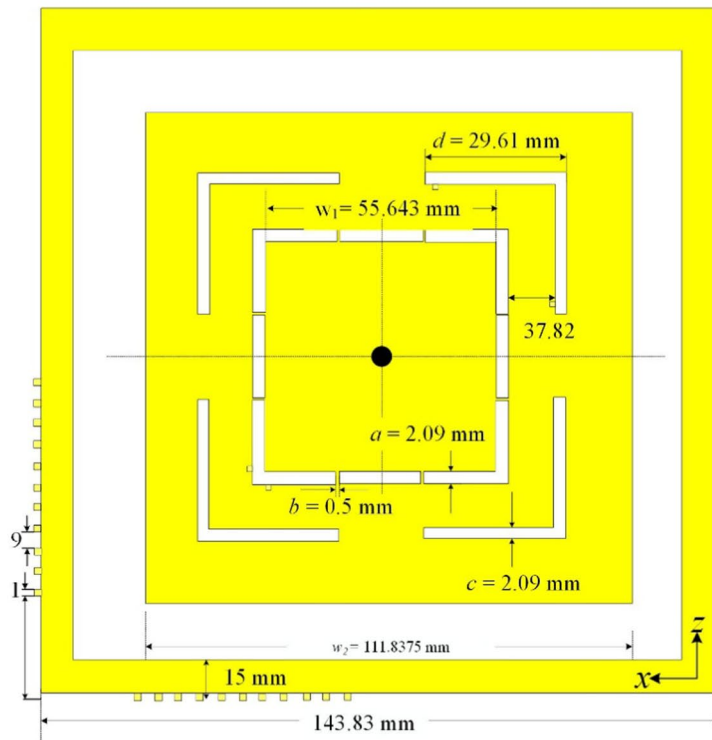


Fig. 3. A switched beam antenna at 0.6 GHz and 2.6 GHz (a) structure (b) S11 and (c) radiation pattern.

Figure 4 illustrates the implementation and results of the strategies, showing how changes to the antenna structure result in better radiation patterns and lower back lobe emissions. Figure 4b through e show the comprehensive, step-by-step design procedure for including parasitic rings and implementing patch etching. Each panel describes a distinct phase of the antenna structure alterations. To further illustrate these effects, current surface distributions for the different configurations have been added to provide a clearer understanding of how the shorted circuits influence the current flow on the antenna patch, as shown in Fig. 5. These surface current plots highlight the changes in current density, showing how the energy is redirected to achieve the desired beam steering and back lobe suppression.

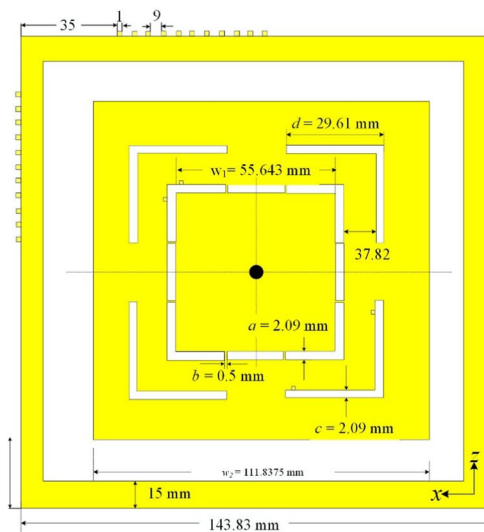


(a)

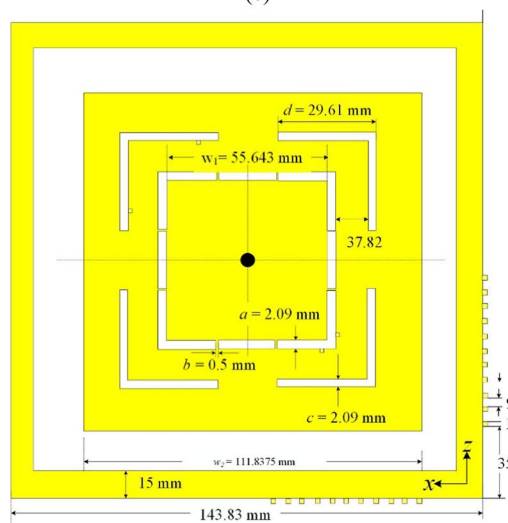


(b)

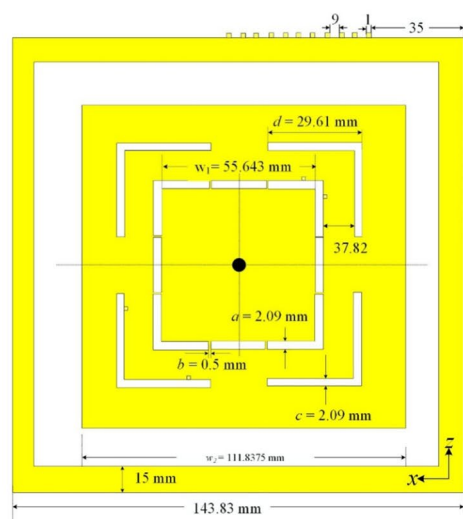
Fig. 4. Configurations of a switched beam antenna with enhanced back lobe suppression: (a) Parasitic rings and patch etching techniques (b) shorted circuit case 1, (c) shorted circuit case 2, (d) shorted circuit case 3, and (e) shorted circuit case 4.



(c)



(d)



(e)

Fig. 4. (continued)

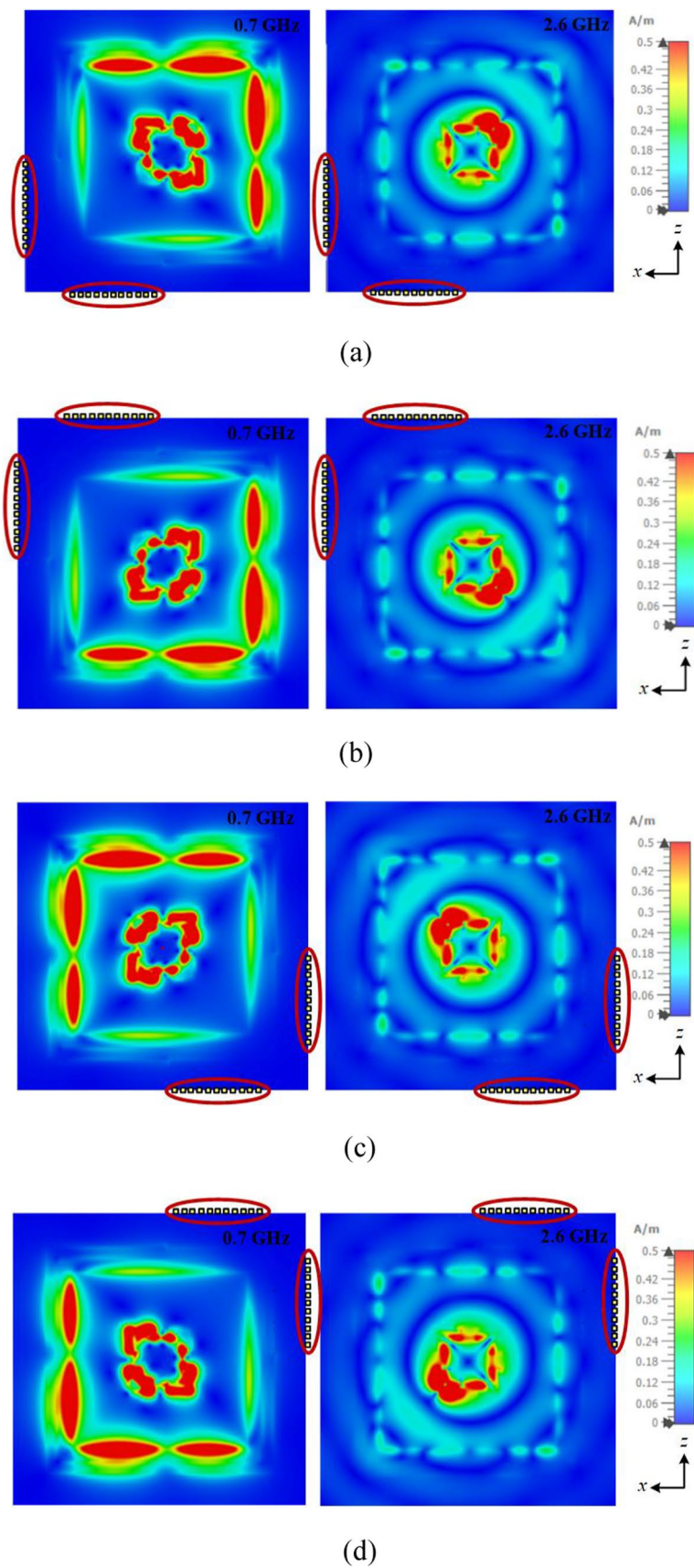


Fig. 5. Surface current of switched beam antenna with enhanced back lobe suppression: (a) case 1, (b) case 2, (c) case 3, and (d) case 4.

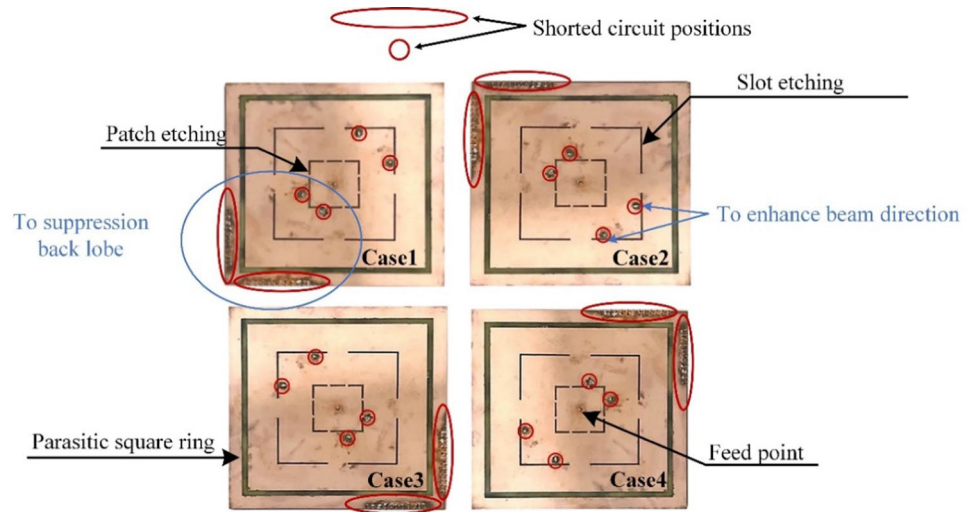


Fig. 6. Prototype of a switched beam antenna with enhanced back lobe suppression.

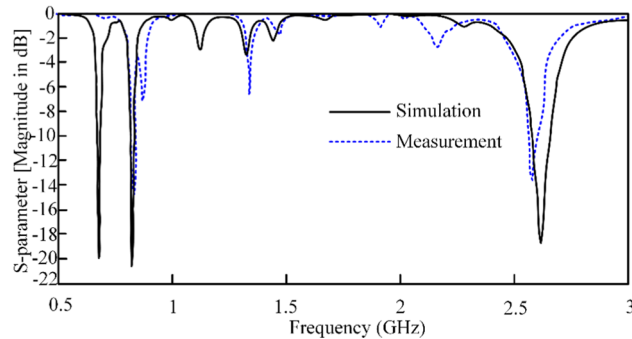


Fig. 7. S_{11} of switched beam antenna with enhanced back lobe suppression.

Figure 6 displays a prototype of a switched beam antenna using back lobe reduction approaches for four scenarios. In this work, the different shorting stubs are employed to control or switch the radiation pattern beam direction. However, this design does not incorporate active components, such as PIN diodes, for dynamic reconfigurability. Instead, the stubs are manually configured to investigate the antenna's performance under different beam-switching scenarios. Future iterations of this design could incorporate PIN diodes or other active switching mechanisms to enable real-time beam reconfigurability. By integrating a DC bias circuit, these components would allow for dynamic control over the stub states, facilitating seamless switching between beam directions without manual intervention. Moreover, the S_{11} results are presented in Fig. 7. A single-patch antenna of the proposed design is inherently limited to providing a narrow bandwidth which makes broadband impedance matching challenging. To overcome this limitation, advanced techniques such as stacked patch structures⁴⁵ and metamaterial-based structures^{46,47} have been proposed. These approaches are particularly suitable for this research as they align with critical design objectives, including bandwidth enhancement and compact form factors for 5G applications. By strategically incorporating these methods, significant improvements in antenna performance may be achieved, ensuring optimized operation across the desired frequency ranges.

Figure 8a through d show the radiation patterns for cases 1 through 4, providing detailed results. In case 1, the back lobes are greatly reduced at 225 degrees, while the main beam is oriented at 45 degrees. In case 2, the back lobes are effectively eliminated at 315 degrees, while the primary beam points toward 135 degrees. In case 3, the lower back lobes are oriented at 135 degrees, and the main beam is oriented at 315 degrees. Finally, in case 4, the main beam is oriented at 225 degrees, successfully minimizing back lobes at 45 degrees. The efficiency of the design improvements is confirmed by these illustrations, which show the antenna's consistent ability to direct the primary beam in line with the shorted circuits on the etched patch. Table 1 offers a clear reference for comprehensive technical information by succinctly summarizing the individual parameter values for our proposed antenna design. The various shorted circuit positions are designed to influence the antenna's beam-steering capability and back lobe suppression. By altering the current distribution on the patch, these shorted circuits enable precise control over the radiation pattern, ensuring that the main beam is oriented towards the desired directions 45°, 135°, 225°, and 315° while minimizing back lobe radiation. This method significantly enhances the antenna's directivity and improves its performance in dense communication environments, where

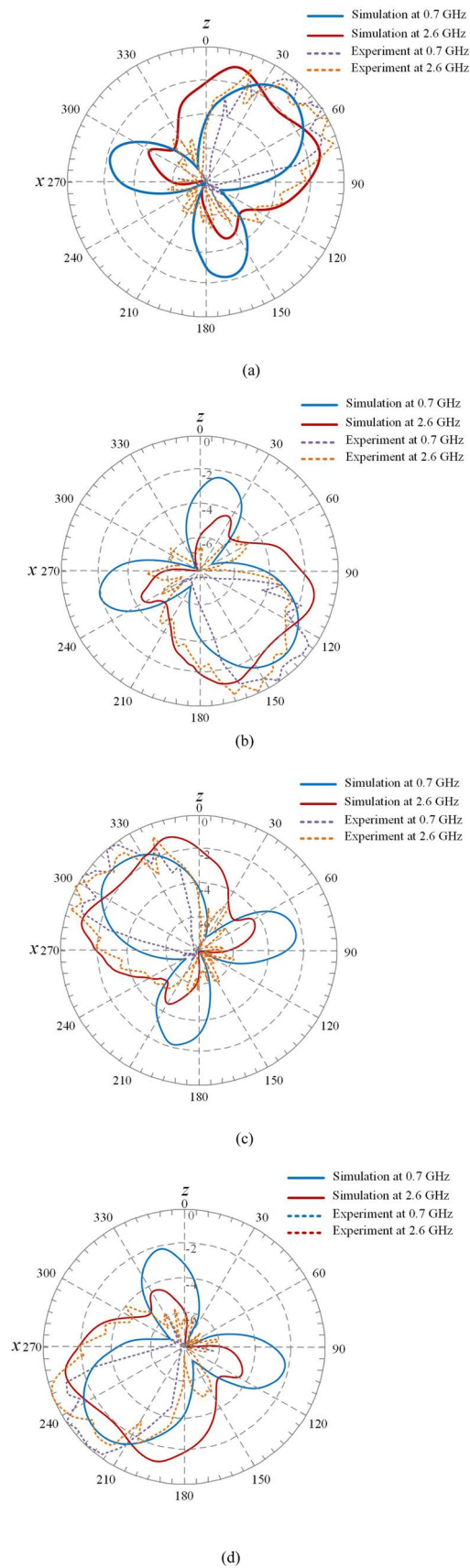


Fig. 8. Radiation pattern of switched beam antenna with enhanced back lobe suppression: (a) case 1, (b) case 2, (c) case 3, and (d) case 4.

Parameters	Size (mm)
Length slot square patch (w_1)	55.643
Length square patch (w_2)	111.8375
Width of ground plane	143.8375
Length of slot etching (d)	29.61
Width of slot square patch (a)	2.09
Gap of slot square patch (b)	0.5
Width of patch etching (c)	2.09
Gap between patch and square parasitic ring	17
Width of square parasitic ring	15

Table 1. Characterizing the parameter values of the antenna.

reducing interference is crucial. This demonstrates how radiation pattern measurements effectively suppress back lobes. Significant reduction in back lobe intensity is observed at the shorted circuit locations along the edges of the square parasitic ring, with all cases consistently performing well at both 0.7 GHz and 2.6 GHz. Due to the absence of a fully anechoic chamber, our measurements were performed in a non-ideal test environment, which can produce minor bifurcations at the apex of the main lobe. Such artifacts result from residual reflections off nearby objects, slight irregularities in the chamber walls, and external electromagnetic interference. Small misalignments during antenna setup and fabrication tolerances may also shift measured patterns away from the simulated results. To mitigate these effects, we recommend averaging multiple sweeps in the current setup and, whenever possible, carrying out future tests in a fully anechoic chamber to reduce environmental distortions and ensure repeatable, reliable results.

The impact of these configurations on the antenna's performance was evaluated through both simulations and practical measurements. The simulation results confirmed that the shorted circuits effectively modify the radiation pattern by concentrating the radiated energy in the desired directions and suppressing unwanted back lobes. The practical measurements aligned closely with the simulated data, demonstrating high beam-switching efficiency and consistent gain values across different configurations.

Comparative analysis and performance validation

Table 2 provides a thorough comparison of our proposed switched beam antenna with several previously published antennas of comparable types, concentrating on factors such as resonance frequency, number of antenna elements, switched beam, reduction procedure, and antenna gain. With its outstanding versatility, the proposed antenna can function at both 2.6 GHz and 0.7 GHz, successfully covering low- and mid-band frequencies necessary for 5G networks in Thailand. The two carrier frequencies are basically integrated into current wireless and cable distribution systems: the 0.7 GHz band (LTE Band 28) provides extensive, long-range coverage for rural and suburban LTE macrocells and intersects with the upper segment of the 54–862 MHz CATV spectrum, enabling in-building cable/Wi-Fi redistribution and prospective converged services. Similarly, the 2.6 GHz band (LTE Bands 7 and 41) has emerged as a global standard for high-capacity LTE and fixed wireless access implementations. Consequently, an antenna that incorporates both 0.7 GHz and 2.6 GHz can be seamlessly retrofitted to existing CATV backhaul links and LTE small cells, while also ensuring preparedness for future 5G non-standalone (NSA) and standalone (SA) enhancements. This operational range distinguishes it from the wider frequency ranges discussed in the literature, including the 2.45 GHz¹⁴, the 28 and 38 GHz dual-band capabilities¹⁵, and the wide frequency coverage¹⁷ from 7.071 GHz to 14.469 GHz. Some designs, as demonstrated in^{27,31}, and⁴², concentrate on specific frequencies such as 1.575 GHz, which serve a broad range of resonant frequency applications. The dual-band microstrip square patch antenna design³⁶, carefully developed to target the crucial frequencies of 0.705 GHz and 2.615 GHz essential for boosting 5G communication efficiency in Thailand, is the reason behind our antenna's exceptional flexibility. There is a comparable pattern in^{8,48–50}. Our proposed antenna uses a simplified single-element design, in contrast to the more intricate multi-element and array configurations characteristic of the designs suggested in^{14,15,28}, and²⁹. This design method is unique in that it integrates numerous advanced features into a single layer, mirroring the simplicity summarized in^{16,17,23,25–27,30,31}, and⁴². The utilization of parasitic rings, etching slots, and well-placed shorted circuits are important achievements.

Our single-element switching beam antenna's advanced back lobe suppression and dynamic beam steering capabilities are made possible by its sophisticated design, which is essential for achieving high transmission efficiency in 5G. With accurate adjustments at 45°, 135°, 225°, and 315°, the proposed antenna's beam-switching capacity equals the performance of cutting-edge designs as suggested in^{15,17}, and²³. This feature highlights the antenna's outstanding directional control efficiency with the least amount of switching mechanisms. Some designs, on the other hand, exhibit a wider range of beam-switching capacities; these include the fundamental 90°, 30°, and 0° configurations in¹⁴ as well as the various azimuthal options in⁴². This variety shows the various approaches used to achieve directed control. The unique feature of our design is the incorporation of advanced shorted circuit techniques into our switched beam antenna. This allows for accurate and adaptable beam steering, which is essential for efficiently addressing 5G communication scenarios. There is a comparable pattern in^{12,51}. The number of intricate procedures described in the literature pales in comparison to the back lobe suppression techniques used in our proposed antenna, which make use of parasitic rings, precise etching, and strategically

Reference	Resonant frequency (GHz)	Number of elements	Switched beam (degree)	Reduction type	Gain (dBi)	Total dimension	Design method	Complexity	Application
14	2.45	Array	0/30/90	-	8	61.1 cm×33.56 cm	Switched parasitic array antennas with adaptive beam steering	Moderate	5G/IoT networks
15	28 and 38	Array	0/10/350	-	12 and 13	22.6 cm×22.6 cm×16 cm	Octagonal prism structure with dual-band, dual-polarized MIMO antenna arrays	High	5G base stations
16	3.5, 3.6, 5.2, 5.8	Single	135/315 ± 30 and 45/225 ± 30	-	2.22 @ 6 GHz, 3.93 @ 8 GHz, and 2.87 @ 10 GHz	9 cm×9 cm×1.67 mm	Beam-switching mechanism using shorted circuits at specific edges of the SSRR	High	5G systems
17	7.071, 9.006, 9.321, 9.906, 10.428, 10.718, 12.967, 13.057, and 14.469	Single	45/225 ± 5 and 135/315 ± 5	-	6.41	6 cm×6 cm×1.67 cm	Multiband switched beam antenna using SSRR	Moderate	5G multiband communication
23	2.4	Five	45°, 135°, 225°, and 315°	-	5.17	30 mm×30 mm×5.5 cm	Combinational parasitic loading method (CPLM)	Low	Wireless networks
26	2.45	Single	-	High-impedance surface	8.5	14 cm×15 cm×0.16 cm	Integration of HIS around the patch antenna	Moderate	Wi-Fi performance
27	1.575	Single	-	Slotted ground choke	6	9 cm×9 cm×0.66 cm	Slotted ground choke	Low	GPS applications
28	5.8	Array	-	DGS	N/A	7 cm×6.42×0.17 cm	DGS with a dumbbell shape	Moderate	Wireless communication
29	9.1	Array	-	DGS	10.09	N/A	DGS at the T-junctions of the feedline network	High	Satellites, missiles, aircraft
30	37.5 to 43.5	Single	-	Dielectric lens (DL)	9	2.38 cm×0.79 cm×0.06 cm	DL and corrugations	High	Compact 5G systems
31	1.575	Single	-	Shorting pins	6.4	4.04 cm×2.82 cm×0.16 cm	Shorting pins	Low	Mobile/Wi-Fi antennas
42	1.575	Array	Five different azimuthal locations	Conductive sleeve	6.4	52 cm×10 cm×0.3 cm	Asymmetrical positioning of microstrip antenna elements relative to the ground plane	Moderate	GNSS systems
The proposed antenna	0.7 and 2.6	Single	45°, 135°, 225°, and 315°	Parasitic rings, Etching slots, shorted circuits	5.39 and 8.35	14.3 cm×14.3 cm×1.74 cm	Parasitic rings, Etching slots, shorted circuits	Moderate	5G networks in urban environments

Table 2. Comparison of literature.

positioned shorted circuits. A few prominent instances are the use of dielectric lenses in³⁰, slotted ground chokes in²⁷, high-impedance surfaces in²⁶, cylindrical copper wires in²⁵, and Defected Ground Structures (DGS) in^{28,29}. Our approach strikes a harmonic balance between improved performance and easier manufacturability by avoiding these complex techniques. Our dual band switching beam antennas carefully designed back lobe suppression procedures, which guarantee both optimal performance and increased production efficiency, enable this streamlined approach. The proposed antenna attains noteworthy gain values of 5.39 dBi at 0.705 GHz and 8.35 dBi at 2.615 GHz, demonstrating strong performance for a compact, single-element design. When compared to gains observed in the literature, which range from 2.22 dBi at 6 GHz in¹⁶ to 13.51 dBi in²⁴, these numbers are competitive. The effectiveness of our antenna design is also noteworthy in contrast to the more intricate structures suggested in^{15,25}, and²⁹, as it achieves such increases with a simpler configuration. The deliberate placement of shorting pins at slot etchings in the main beam direction, a crucial component of back lobe suppression techniques for dual-band switching beam antennas, further improves performance. By greatly increasing directivity and reducing interference, this integration guarantees that our antenna not only satisfies but also surpasses performance requirements. This design's low profile, ease of manufacture, and ability to switch beams while maintaining high gain over two resonant frequencies are its main features. Moreover, the back lobe reduction techniques used are simple and effective, enhancing performance without adding complexity to the design. Despite these advantages, the lower and mid-band frequencies, that is, 2.6 GHz and 0.7 GHz, are the main subjects of this research on the 5G antenna at present. To fully implement 5G, it would be advantageous to extend the design's reach to include the high-band spectrum, specifically the 24 GHz to 40 GHz band. Improving the antenna's performance in this higher frequency range would be in line with the wider demands of 5G technology, guaranteeing better coverage and faster data transfer rates in crowded cities where high-band frequency utilization/n is essential.

Conclusions

The design and construction of a single-element, dual-band switching beam antenna that satisfies the demanding standards of 5G wireless communications are successfully presented in this work. The critical frequency ranges for 5G applications in Thailand are 0.7 GHz and 2.6 GHz, where the proposed antenna performs well. Significant improvements in signal clarity and interference reduction were obtained by incorporating advanced back lobe suppression techniques, such as patch etching, parasitic elements, and strategically positioned short circuits. The dynamic beam-steering capacity of the antenna, which allowed for directional switching at 45°, 135°, 225°, and 315°, was thoroughly verified through simulations and empirical testing. The results demonstrated excellent beam-switching performance, showing gains of 5.39 dBi at 0.7 GHz and 8.35 dBi at 2.6 GHz. These findings offer a robust solution for enhancing 5G network coverage and reliability, especially in crowded urban areas.

This research provides valuable insights into antenna designs for future wireless technologies. A significant improvement over conventional techniques is the novel use of parasitic components and patch etching for back lobe suppression. This design is a practical and affordable option for 5G networks, ensuring simple integration into existing systems while providing enhanced performance. In conclusion, the proposed antenna shows great promise for improving 5G communication networks. Future efforts may focus on extending the design's coverage to higher frequency bands, specifically in the range of 24 GHz to 40 GHz, to fully meet the extensive specifications of 5G technology. Such developments would ensure improved coverage and data transmission speeds, particularly in crowded urban areas where high-band frequency usage is essential.

Data availability

The datasets used and/or analyzed during the current study available from the corresponding author on reasonable request.

Received: 4 September 2024; Accepted: 4 August 2025

Published online: 12 August 2025

References

1. Denis, A. Overview of ITU-T Activities on 5G/IMT-2020, in ITU Committed to Connecting the World, 2019. [Online]. <https://www.itu.int>
2. Sanou, B. Setting the Scene for 5G: Opportunities & Challenges, in 2018 International Telecommunication Union, 2018. [Online]. <https://www.itu.int>
3. Lee, C. & Basics, G. in 2017 International Telecommunication Union, [Online]. (2017). <https://www.itu.int>
4. Carugi, M. Key Features and Requirements of 5G/IMT-2020 Networks, in 2018 ITU Arab Forum on Emerging Technologies, 2018. [Online]. <https://www.itu.int>
5. Nordrum, A. & Clark, K. Everything you need to know about 5G. *IEEE Spect. Technol. Eng. Sci. News* (2019).
6. Gross Frank, B. Smart antenna. In *Smart Antenna for Wireless Communications with MATLAB*, 1st ed. 207–266. (McGraw-Hill, 2005).
7. Zooghby, A. E. Fixed beam smart antenna systems and adaptive array systems. In *Smart Antenna Engineering*, 83–158 (Artech House Publishers, 2005).
8. Chaipanya, P. et al. Dual band switched beam textile antenna for 5G wireless communications. *CMC Comput. Mater. Continua* **73**(1), 181–198 (2022).
9. Chaipanya, P., Santalunai, N. & Santalunai, S. A design of a single element switched beam antenna on mushroom-like EBG structures. *Przegląd Elektrotechniczny* **97**(11), 35–39 (2021).
10. Olk, E. & Powell, D. A. Huygens metasurface lens for W-Band switched beam antenna applications. *IEEE Open. J. Antennas Propag.* **1**, 290–299 (2020).
11. Chen, Z., Qiao, H., Chen, Q. & Chen, X. A wideband and high-gain switched-beam antenna system using active frequency selective surface. *IET Microwave Antennas Propag.*, **17**(14), 1056–1061 (2023).
12. Morshed, K. M., Karmokar, D. K., Esselle, K. P. & Matekovits, L. Beam-Switching antennas for 5G millimeter-wave wireless terminals. *Sensors*, **23**(14), Art. 6285 (2023).
13. Seman, N., Syahira, N., Suhaimi, M. & Chua, T. H. 26 ghz phase Shifters for multi-beam Nolen matrix towards fifth generation (5G) technology. *Bullet. Electr. Eng. Inform.* **8**(3), 1028–1035 (2019).
14. Kausar, A., Mehrpouyan, H., Sellathurai, M., Qian, R. & Kausar, S. Energy efficient switched parasitic array antenna for 5G networks and IoT. In *Loughborough Antennas & Propagation Conference (LAPC)*, 1–5 (Loughborough, UK, 2016).
15. Elhabbash, T. & Skaik, T. Design of dual-band dual-polarized MIMO antenna for mm-wave 5G base stations with octagonal prism structure. In *2019 IEEE 7th Palestinian International Conference on Electrical and Computer Engineering (PICECE)*, 1–6 (Gaza, Palestine, 2019).
16. Chaipanya, P., Punchin, M., Prasoptunya, N. & Phothong-ngam, W. Low cost multiband switched beam antenna for 5G applications. In *2018 International Electrical Engineering Congress (iEECON)*, 1–4 (Krabi, Thailand, 2018).
17. Chaipanya, P., Punchin, M., Prasoptunya, N. & Phothong-Ngam, W. A single element of multiband switched beam antenna for 5G applications. *Int. J. Electr. Comput. Eng. (IJECE)* **12**(3), 2733–2742 (2022).
18. Chung, M. A., Lin, C. W. & Yang, C. W. A Low-Cost Four-Directional beamforming switched butler matrix network antenna for 5G NR applications. *IEEE Access* **12**, 42949–42960 (2024).
19. Bembarca, A., Setti, L., Tribak, A., Tizyi, H. & Ouahabi, M. E. A novel wideband beamforming antenna for 5G applications by eliminating the phase Shifters and crossovers from the butler matrix. *Progress Electromagnet. Res. C.* **133**, 51–63 (2023).
20. Zidour, A. et al. Wideband endfire antenna array for 5G mmWave mobile terminals. *IEEE Access* **12**, 39926–39935 (2024).
21. Kim, Y. J., Kim, Y. B., Dong, H. J., Cho, Y. S. & Lee, H. L. Compact switched-beam array antenna with a butler matrix and a folded ground structure. *Electronics* **9**(1), 1–12 (2020).
22. Cafsi, M. A. E., Nedil, M., Osman, L. & Gharsallah, A. The design of a 360° switched-beam-base station antenna, *Antenna Arrays and Beam-formation*. In *InTech* (2017).
23. Mofolo, M. R. O., Lysko, A. A., Olwal, T. O. & Clarke, W. A. Beam steering for circular switched parasitic arrays using a combinational approach, In *IEEE Africon '11, Victoria Falls, Zambia*, 1–6 (2011).
24. Lee, S., Lee, Y. & Shin, H. A 28-GHz switched-beam antenna with integrated butler matrix and switch for 5G applications. *Sensors* **21** (15), 1–14 (2021). Art. 5128.
25. Zahar, Z. & Bin Ain, M. F. Backlobe reduction of air substrate circular patch antenna for 5G applications. In *11th International Conference on Robotics, Vision, Signal Processing and Power Applications*, 948–954 (2022).

26. Wang, D., Wei, X., Zhang, J., Shu, Y. & Yang, D. Back lobe reduction of patch antenna by using high-impedance surface (Invited). In *IET International Radar Conference 2015*, 1–4 (Hangzhou, 2015).
27. Lim, W. G., Jang, H. & Yu, J. W. New method for back lobe suppression of microstrip patch antenna for GPS. In *The 40th European Microwave Conference*, 679–682 (Paris, France, 2010).
28. Alias, H., Ali, M. T., Ramli, S. S. N., Sulaiman, M. A. & Kayat, S. A back lobe reduction of aperture coupled microstrip antenna using DGS. In *10th International Conference on Electrical Engineering/Electronics, Computer, Telecommunications and Information Technology*, 1–5 (Krabi, Thailand, 2013).
29. Lakshmana Kumar, V. N., Satyanarayana, M. & Singh, S. P. A novel technique for sidelobe and backlobe reduction in rectangular microstrip antenna array using defected ground structures. *Int. J. Appl. Eng. Res.* **13**(22), 15961–15966 (2018).
30. Dixit, A. S., Kumar, S. & Urooj, S. A constant gain and miniaturized antipodal Vivaldi antenna for 5G communication applications. *Comput. Mater. Continua* **73**(3), 4909–4921 (2020).
31. Kurup, H. B., Antony, D., Rajan, V. & Rodrigues, S. Analysis and implementation of shorting pins in microstrip patch antenna for SAR reduction. *Physica Scr.* **99**, no. 3, Art. 035539 (2024).
32. Din, I. et al. High performance antenna system in MIMO configuration for 5G wireless communications over sub-6 GHz spectrum. *Radio Sci.* **58**(10), 1–22 (2023).
33. Chaipanya, P. Single element switched beam antenna utilizing parasitic elements for back lobe reduction. In *ICTCE '17: Proceedings of the 2017 International Conference on Telecommunications and Communication Engineering*, 5–19 (2017).
34. Ali, M. T. et al. A Reconfigurable planar antenna array (RPAA) with back lobe reduction. In *2010 International Workshop on Antenna Technology (iWAT)*, 1–4 (Lisbon, Portugal, 2010).
35. Karami, M., Sadeghzadeh, R. A., Noferesti, M. & Sharifi, M. Suppressed back-lobe SIW-fed MPA array for 60 GHz wireless communication. In *9th European Conference on Antennas and Propagation (EuCAP)*, 1–4 (Lisbon, Portugal, 2015).
36. Chaipanya, P., Rattanakriengkai, P., Potup, P. & Lapourailers, L. A dual-band single-feed switched beam antenna for WLAN. *Int. J. Electron. Telecommun.* **63**(4), 405–408 (2017).
37. Balanis, C. A. *Antenna Theory. Analysis and Design (3rd Edition)* (A John Wiley & Sons, Inc., 2015).
38. Kim, G. & Kim, S. Design and analysis of dual polarized broadband microstrip patch antenna for 5G mm wave antenna module on FR4 substrate. *IEEE Access* **9**, 64306–64316 (2021).
39. Liu, R., Ma, K., Yan, N., Wang, Y. & Wu, Y. An FR4-based miniaturized high-efficiency double-sided SISL longitudinal slot antenna array for 5g millimeter-wave applications. *IEEE Trans. Antennas Propag.* **72**(7), 6099–6104 (2024).
40. Singh, U., Mishra, R., Dual-Band, A. & High-gain substrate integrated waveguide slot antenna for 5G application. *Progress Electromagnet. Res. C.* **119**, 191–200 (2022).
41. Sakulchat, S., Ruengwaree, A., Naktong, W., Unahalekhaka, P. & Promput, S. Low-cost high gain sea pimple-shaped dual band monopole antenna for mobile 4G/5G/LTE41/WLAN application. *Progress Electromagnet. Res. C.* **140**, 41–51 (2024).
42. Silveira, E. S., Nascimento, D. C. & Tinoco-S, A. F. Design of microstrip antenna array with suppressed back lobe. *J. Microwaves Optoelectron. Electromagn. Appl.*, **16**(2) (2017).
43. Schlub, R. & Thiel, D. V. Switched parasitic antenna on a finite ground plane with conductive sleeve. *IEEE Trans. Antennas Propag.* **52**(5), 1343–1347 (2004).
44. Guha, D., Biswas, M. & Antar, Y. M. M. Microstrip patch antenna with defected ground structure for cross polarization suppression. *IEEE Antennas Wirel. Propag. Lett.* **4**, 455–458 (2005).
45. Chen, J. X., Zhou, J., Cai, J. & Yang, W. W. Bandwidth-enhanced frequency-agile stacked patch antenna sharing common tuning element. *IEEE Antennas Wirel. Propag. Lett.*, 1–5 (2024).
46. Si, L., Jiang, H., Lv, X. & Ding, J. Broadband extremely close-spaced 5G MIMO antenna with mutual coupling reduction using metamaterial-inspired superstrate. *Opt. Express* **27**(3), 3472–3482 (2019).
47. Vallappil, A. K., Rahim, M. K. A., Khawaja, B. A. & Iqbal, M. N. A miniaturized metamaterial-loaded switched-beam antenna array system with enhanced bandwidth for 5G applications. *IEEE Access* **3**, 6684–6697 (2024).
48. Ahmad, I. et al., Design and experimental analysis of multiband compound reconfigurable 5G antenna for Sub-6 GHz wireless applications. *Wireless Commun. Mob. Comput. Art* 5588105 (2021).
49. 6 GHz in the 5G Era – global insights on 5925–7125 Mhz, GSMA. [Online]. July (2022). <https://www.gsma.com/connectivity-for-good/spectrum/wp-content/uploads/2022/07/6-GHz-in-the-5G-Era.pdf>
50. Abdul-Rahman, E. & Aloï, D. N. Design of a 5G sub-6 GHz vehicular cellular antenna element with consistent radiation pattern using characteristic mode analysis. *Sensors* **21**(22), Art. 8862 (2022).
51. Lee, S., Lee, Y. & Shin, H. A 28-GHz switched-Beam antenna with integrated butler matrix and switch for 5G applications. *Sensors*, **21**, 15 Art. 5128 (2021).

Acknowledgements

This work was supported by Srinakharinwirot University (SWU) and Faculty of Engineering, SWU, Thailand.

Author contributions

Conceptualization, P.C., K.P., S.S., and N.S.; methodology, P.C., W.K., N.W., C.W., N.T, W.S., K.P., S.S., and N.S.; investigation, P.C., W.K., N.W., C.W., N.T, W.S., K.P., S.S., and N.S.; formal analysis, P.C., W.K., N.W., C.W., N.T, W.S., K.P., S.S., and N.S.; writing—original draft, P.C., K.P., S.S., and N.S.; writing—review and editing, P.C., K.P., S.S., and N.S.; supervision, P.C., K.P., S.S., and N.S.; funding acquisition, P.C., All authors have read and agreed to the published version of the manuscript.

Funding

This work was supported by Srinakharinwirot University (SWU) and Faculty of Engineering, SWU, Thailand. through the research grant No. 175/2566.

Declarations

Competing interests

The authors declare no competing interests.

Declaration of generative AI and AI-assisted technologies in the writing process

During the preparation of this work, the authors used AI-assisted technologies to improve only language and readability. After using this tool/service, the authors reviewed and edited the content as needed and takes full responsibility for the content of the publication.

Additional information

Correspondence and requests for materials should be addressed to P.C. or N.S.

Reprints and permissions information is available at www.nature.com/reprints.

Publisher's note Springer Nature remains neutral with regard to jurisdictional claims in published maps and institutional affiliations.

Open Access This article is licensed under a Creative Commons Attribution-NonCommercial-NoDerivatives 4.0 International License, which permits any non-commercial use, sharing, distribution and reproduction in any medium or format, as long as you give appropriate credit to the original author(s) and the source, provide a link to the Creative Commons licence, and indicate if you modified the licensed material. You do not have permission under this licence to share adapted material derived from this article or parts of it. The images or other third party material in this article are included in the article's Creative Commons licence, unless indicated otherwise in a credit line to the material. If material is not included in the article's Creative Commons licence and your intended use is not permitted by statutory regulation or exceeds the permitted use, you will need to obtain permission directly from the copyright holder. To view a copy of this licence, visit <http://creativecommons.org/licenses/by-nc-nd/4.0/>.

© The Author(s) 2025, corrected publication 2025